Oligoribonuclease is the primary degradative enzyme for pGpG in *Pseudomonas aeruginosa* that is required for cyclic-di-GMP turnover

Mona W. Orr[a,b,c], Gregory P. Donaldson[a,c], Geoffrey B. Severin[d], Jingxin Wang[e], Herman O. Sintim[e], Christopher M. Waters[f], and Vincent T. Lee[a,c,1]

[a]Department of Cell Biology and Molecular Genetics, University of Maryland, College Park, MD 20742; [b]Biological Sciences Graduate Program, University of Maryland, College Park, MD 20742; [c]Maryland Pathogen Research Institute, University of Maryland, College Park, MD 20742; [d]Department of Biochemistry and Molecular Biology, Michigan State University, East Lansing, MI 48824; [e]Department of Chemistry and Biochemistry, University of Maryland, College Park, MD 20742; and [f]Department of Microbiology and Molecular Genetics, Michigan State University, East Lansing, MI 48824

Edited by E. Peter Greenberg, University of Washington, Seattle, WA, and approved July 31, 2015 (received for review April 14, 2015)

The bacterial second messenger cyclic di-GMP (c-di-GMP) controls biofilm formation and other phenotypes relevant to pathogenesis. Cyclic-di-GMP is synthesized by diguanylate cyclases (DGCs). Phosphodiesterases (PDE-As) end signaling by linearizing c-di-GMP to 5′-phosphoguanylyl-(3′,5′)-guanosine (pGpG), which is then hydrolyzed to two GMP molecules by yet unidentified enzymes termed PDE-Bs. We show that pGpG inhibits a PDE-A from *Pseudomonas aeruginosa*. In a dual DGC and PDE-A reaction, excess pGpG extends the half-life of c-di-GMP, indicating that removal of pGpG is critical for c-di-GMP homeostasis. Thus, we sought to identify the PDE-B enzyme(s) responsible for pGpG degradation. A differential radial capillary action of ligand assay-based screen for pGpG binding proteins identified oligoribonuclease (Orn), an exoribonuclease that hydrolyzes two- to five-nucleotide-long RNAs. Purified Orn rapidly converts pGpG into GMP. To determine whether Orn is the primary enzyme responsible for degrading pGpG, we assayed cell lysates of WT and Δ*orn* strains of *P. aeruginosa* PA14 for pGpG stability. The lysates from Δ*orn* showed 25-fold decrease in pGpG hydrolysis. Complementation with WT, but not active site mutants, restored hydrolysis. Accumulation of pGpG in the Δ*orn* strain could inhibit PDE-As, increasing c-di-GMP concentration. In support, we observed increased transcription from the c-di-GMP–regulated *pel* promoter. Additionally, the c-di-GMP–governed auto-aggregation and biofilm phenotypes were elevated in the Δ*orn* strain in a *pel*-dependent manner. Finally, we directly detect elevated pGpG and c-di-GMP in the Δ*orn* strain. Thus, we identified that Orn serves as the primary PDE-B enzyme that removes pGpG, which is necessary to complete the final step in the c-di-GMP degradation pathway.

cyclic di-GMP | oligoribonuclease | pGpG | PDE-B | nanoRNase

Cyclic-di-GMP (c-di-GMP) is a phylogenetically widely used bacterial second messenger (1). Cyclic-di-GMP is synthesized by diguanylate cyclase enzymes (DGC) that contain the GGDEF domain (2, 3). Once synthesized, the c-di-GMP binds to intracellular receptors to decrease motility and increase biofilm formation, contributing to the virulence of several pathogens (1, 4–7). Cyclic-di-GMP signaling is terminated by phosphodiesterases (PDE-A) that linearize it into pGpG, which is then hydrolyzed into GMP by an unknown phosphodiesterase termed PDE-B (2). Bacteria encode two structurally unrelated PDE-As: one containing the EAL domain (8–10) and a second containing the HD-GYP domain (11). The overexpression of GGDEF domain DGCs elevates c-di-GMP and c-di-GMP–regulated processes (8, 12); conversely, overexpression of the EAL and HD-GYP domain PDE-As decreases c-di-GMP and c-di-GMP–regulated processes (8, 13–15). These c-di-GMP synthesizing and degrading domains are commonly linked to sensory and signal transduction domains (1, 16), thereby allowing synthesis and degradation of c-di-GMP in response to environmental changes.

In addition to regulation by extracellular signals, c-di-GMP homeostasis is subject to feedback inhibition. Crystal structures of the DGCs PleD from *Caulobacter crescentus* and WspR from *Pseudomonas aeruginosa* show that c-di-GMP binds to an RxxD domain I-site to inhibit c-di-GMP synthesis (17, 18). Additionally, the *Xanthomonas campestris* XCC4471 DGC lacking an RxxD motif can also be inhibited by excess c-di-GMP through c-di-GMP binding to and occluding the active site (19). The linearized c-di-GMP hydrolysis product, 5′-phosphoguanylyl-(3′,5′)-guanosine (pGpG), also plays an active role in cyclic dinucleotide turnover. Purified YfgF from *E. coli*, a PDE-A, is inhibited by excess pGpG through an unknown mechanism (20). Here, we show that the EAL domain PDE-A RocR from the *P. aeruginosa* PA14 strain is also inhibited by excess pGpG via direct competition with c-di-GMP binding in the active site. Accordingly, the addition of excess pGpG results in an increased c-di-GMP half-life in vitro, suggesting that removal of pGpG is required for terminating c-di-GMP signaling.

To elucidate the mechanism of c-di-GMP signal termination, we sought to identify the PDE-B(s) responsible for cleaving pGpG. Previously, HD-GYP domain-containing proteins were

Significance

Cyclic-di-GMP (c-di-GMP) is a ubiquitous bacterial second messenger that regulates complex behaviors such as biofilm formation. These behaviors are changed by altering the intracellular concentration of c-di-GMP. Degradation of c-di-GMP occurs by a two-step process in which one set of phosphodiesterases (PDE-As) linearize the molecule into 5′-phosphoguanylyl-(3′,5′)-guanosine (pGpG), followed by hydrolysis by unidentified phosphodiesterases (PDE-Bs) into two GMPs. High levels of pGpG inhibit PDE-As, and thus PDE-B activity is important in maintaining c-di-GMP homeostasis. However, the identity of the PDE-B(s) remained unknown. Using a high-throughput binding screen, we identify oligoribonuclease (Orn) as a putative PDE-B. We demonstrate that Orn is the primary source of PDE-B activity in *Pseudomonas aeruginosa*. Identification of Orn as the primary PDE-B completes the c-di-GMP signaling pathway.

Author contributions: M.W.O., G.P.D., G.B.S., H.O.S., C.M.W., and V.T.L. designed research; M.W.O., G.P.D., G.B.S., and J.W. performed research; G.B.S. contributed new reagents/analytic tools; M.W.O., G.P.D., G.B.S., C.M.W., and V.T.L. analyzed data; and M.W.O., G.B.S., C.M.W., and V.T.L. wrote the paper.

The authors declare no conflict of interest.

This article is a PNAS Direct Submission.

Freely available online through the PNAS open access option.

[1]To whom correspondence should be addressed. Email: vtlee@umd.edu.

This article contains supporting information online at www.pnas.org/lookup/suppl/doi:10.1073/pnas.1507245112/-/DCSupplemental.

proposed to be the PDE-Bs involved in pGpG hydrolysis because they bind pGpG with higher affinity than c-di-GMP (21). However, HD-GYP domain proteins are missing in some genomes that contain other c-di-GMP signaling machinery (1), suggesting that other enzymes must be responsible for PDE-B activity. To identify PDE-B(s), we used a screen based on the differential radial capillary action of ligand assay (DRaCALA) (22, 23) to probe an ORF library of *Vibrio cholerae* El Tor N16961 (24) for proteins that bind pGpG. This screen identified oligoribonuclease (Orn) as a protein that binds pGpG, but not c-di-GMP. Orn is an exoribonuclease that cleaves two- to five-nucleotide-long RNA molecules (25). We found that purified Orn from both *V. cholerae* and *P. aeruginosa* bound and cleaved pGpG. To determine whether Orn is the primary PDE-B in bacteria, we show that whole cell lysates of an *orn* transposon mutant (*orn*::tn) from the *P. aeruginosa* PA14 Non-Redundant Transposon Insertion Mutant Library (26) and an in-frame deletion mutant of *orn* (Δ*orn*) were decreased in pGpG cleaving activity by 25-fold compared with the parental strain. Complementation with WT *orn,* but not active site point mutants, restored pGpG hydrolysis in cell lysates. Thus, loss of *orn* is expected to increase pGpG concentration in vivo and may inhibit PDE-A activity to also elevate c-di-GMP concentrations in the Δ*orn* strain. In support of elevated c-di-GMP in the Δ*orn* strain, we observed three times more activity from the c-di-GMP–responsive *pel* promoter FleQ (27). We also demonstrate that two c-di-GMP–governed phenotypes, biofilm formation (28) and aggregation (29), are enhanced in the Δ*orn* strain and are dependent on the c-di-GMP–regulated PEL exopolysaccharides (30). Using LC-MS/MS, we directly detect higher levels of both pGpG and c-di-GMP in extracts of the Δ*orn* strain compared with WT. Taken together, these results indicate that Orn is the primary PDE-B responsible for degrading pGpG in *P. aeruginosa*.

Results

pGpG Inhibits RocR Phosphodiesterase Activity by Binding to the Active Site. The PDE-A YfgF from *E. coli* is inhibited by the addition of 100 μM of pGpG (20). We asked whether PDE-A inhibition by pGpG is a generalizable phenomenon. The RocR PDE-A from *P. aeruginosa* PA14 was used to determine inhibition by pGpG. In the absence of competitor (Fig. 1*A*), RocR rapidly converts 89% of the radiolabeled c-di-GMP to pGpG within 5 min as measured after separation by TLC. The addition of 100-fold excess of pGpG nearly completely inhibited c-di-GMP linearization (Fig. 1*A*). These results demonstrate that pGpG inhibits PDE-A activity. To determine whether pGpG is competing with c-di-GMP for active site binding in RocR, we performed experiments in which binding of radiolabeled c-di-GMP to purified RocR was assessed in the presence of different unlabeled nucleotide competitors. RocR binds c-di-GMP with a fraction bound of 0.54 ± 0.03 in the absence of competitor, whereas the addition of 50 μM unlabeled pGpG reduced fraction bound to 0.022 ± 0.005 ($P < 0.001$), indicating that pGpG competes for c-di-GMP binding (Fig. 1*B*, black bars). To see whether binding is mutually exclusive, RocR was incubated with radiolabeled pGpG in the presence of the same panel of unlabeled nucleotide competitors (Fig. 1*B*, white bars). The addition of 50 μM c-di-GMP reduced fraction bound from 0.48 ± 0.01 to 0.13 ± 0.03 ($P < 0.001$), indicating that c-di-GMP is also able to prevent pGpG binding. No other nucleotide had a significant effect on fraction of pGpG or c-di-GMP bound to RocR (Fig. 1*B*). Thus, RocR binding to pGpG and c-di-GMP is specific and mutually exclusive. Crystal structures of another EAL domain PDE-A FimX show that pGpG binds in the active site where c-di-GMP cleavage occurs (31). Because the binding is occurring at the same site, the relative affinity of RocR binding to pGpG and c-di-GMP is important to determine whether pGpG competition of c-di-GMP binding could occur in physiological conditions. The dissociation constant (K_d) of RocR binding to pGpG and c-di-GMP was found to be 3.6 ± 0.4 and 0.60 ± 0.07, μM respectively (Fig. 1*C*). The c-di-GMP concentration in WT *P. aeruginosa* has been reported to be up to 11 μM (32). Therefore, rapid turnover of c-di-GMP can yield pGpG concentrations that exceed the K_d for RocR if pGpG is not also quickly removed from the cell.

Excess pGpG Extends c-di-GMP Half-Life in Vitro. Inhibition of RocR by pGpG should effectively increase the half-life of c-di-GMP. To test this in vitro, a coupled DGC and PDE-A reaction was performed to trace the synthesis and linearization of c-di-GMP in the presence of different intermediates in the c-di-GMP biosynthesis and degradation pathways. Specifically, the DGC WspR and PDE-A RocR from *P. aeruginosa* PA14 were incubated with radiolabeled α-^{32}P-GTP in the presence of (*i*) no competitor, (*ii*) GMP, (*iii*) c-di-GMP, or (*iv*) pGpG. The reactions were stopped at different times by the addition of the divalent metal chelator EDTA and heat inactivation. The reaction products were separated by TLC, and intensities of radiolabeled GTP, c-di-GMP, and pGpG were quantified (Fig. 2). In the absence of any competitor, the α -^{32}P-GTP is converted to c-di-GMP, which is then linearized to pGpG. Adding 100-fold excess GMP shows no effect on enzymatic activity, as expected (Fig. 2 *A* and *B*). Addition of excess c-di-GMP inhibited the ability of WspR to convert α-^{32}P-GTP to c-di-GMP, which is consistent with inhibition through binding to

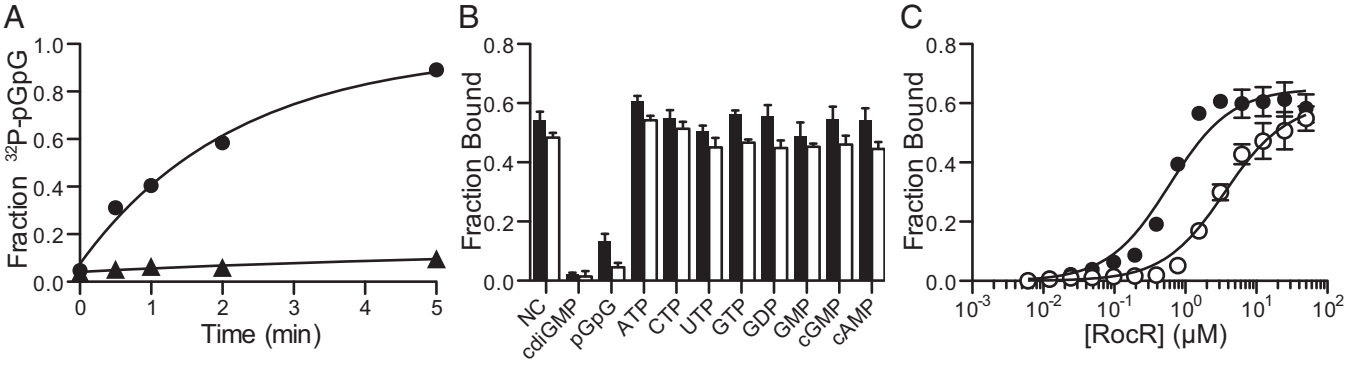

Fig. 1. pGpG inhibits RocR phosphodiesterase activity by competing for c-di-GMP binding in the active site. (*A*) The rate of ^{32}P-pGpG formation from ^{32}P-c-di-GMP hydrolysis by RocR in the absence of competitor (NC, circle) or 500 μM pGpG competitor (triangle). (*B*) The fraction bound of ^{32}P-c-di-GMP (black) or ^{32}P-pGpG (white) to RocR (10 μM) was quantified by DRaCALA in the presence of no competitor (NC) or 500 μM excess unlabeled nucleotide competitor. (*C*) The dissociation constants (K_d) for RocR binding to ^{32}P-c-di-GMP (black) and ^{32}P-pGpG (white) as determined by DRaCALA. All data shown represent the average and SD of triplicate independent experiments.

the I-site (Fig. 2*C*) (17, 18). Most importantly, the addition of excess pGpG reduced the turnover of c-di-GMP (Fig. 2*D*), supporting our hypothesis that elevated concentrations of pGpG can increase the half-life of c-di-GMP by reducing PDE-A activity.

Identification of pGpG Binding Proteins from *V. cholerae* ORF Library. Based on the above results, the PDE-B responsible for hydrolyzing pGpG is critical for completing the c-di-GMP degradation pathway. To identify this enzyme, we used a high-throughput DRaCALA-based screen to interrogate pGpG binding to a library of ORFs (22, 23). The *V. cholerae* El Tor N16961 complete genome ORF library (ORFeome) was used because 97% of the ORFs are represented (24), and *V. cholerae* uses c-di-GMP signaling extensively (33, 34). Each ORF was recombined into two destination vectors with an isopropyl-β-D-1-thiogalactopyranoside (IPTG)-inducible T7 promoter, one containing a 10× histidine N-terminal tag and a second containing a 10× histidine-maltose binding protein (MBP) N-terminal tag. These two libraries were individually introduced into an *E. coli* T7Iq expression strain and arrayed in 96-well plates. Following IPTG induction, whole cell lysates were generated and assayed for binding to pGpG using DRaCALA. The fraction bounds for each ORF tested are listed in Table S1. Positive hits were defined as 3 SDs above the mean fraction bound of the entire library. For validation, each positive hit was repicked from the expression library and reassayed for pGpG binding. The fraction of each ORF bound to pGpG is shown for both ORFeomes with validated hits in color (Fig. 3). A list of hits and their known or predicted functions is provided in Table S2.

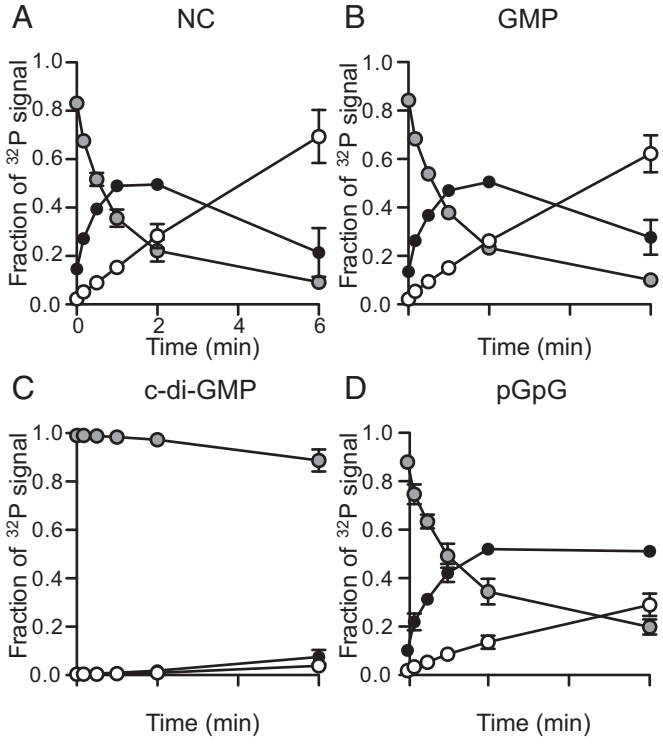

Fig. 2. Excess pGpG extends the half-life of c-di-GMP in an in vitro diguanylate cyclase and phosphodiesterase activity assay. TLC-based quantification of the conversion of ^{32}P-GTP (gray) to ^{32}P-c-di-GMP (black) and ^{32}P-pGpG (white) in a coupled WspR and RocR reaction in (*A*) the absence of competitor (NC), (*B*) 300 μM GMP, (*C*) 300 μM c-di-GMP, or (*D*) 300 μM pGpG. All data shown represent the average and SD of duplicate independent experiments.

The *V. cholerae* ORFeome library includes known c-di-GMP binding proteins: 28 of 31 GGDEF domain proteins (33), all 5 PilZ domain proteins (35), and all 3 c-di-GMP-binding transcription factors (36–38). None of these proteins were identified in this screen, indicating that the assay is specific for pGpG-binding proteins. We expected to identify EAL domain and HD-GYP domain proteins, both of which have been shown to bind pGpG (21, 31). The *V. cholerae* ORFeome library includes 11 of 12 EAL domain proteins encoded in the genome, 9 of 10 dual GGDEF-EAL domain proteins, and all 9 HD-GYP domain proteins (33). Of these, four EAL domain-containing proteins, VC1592, VC1641, VC1652, and VC1710 (Fig. 3, blue dots); four GGDEF-EAL domain containing proteins, VC0653, VC0658, VC2750, and VCA0080 (Fig. 3, green dots); and two HD-GYP domain containing proteins, VCA0681 and VCA0931 (Fig. 3, purple dots), bound pGpG in the screen. Not all EAL or HD-GYP domain ORF lysates showed binding in this system, which could reflect either genuine inability to bind pGpG or low protein expression in *E. coli,* resulting in concentrations below the K_d.

Because pGpG is a two-nucleotide-long RNA, we expected ribonucleases (RNases) to bind as well. The ORFeome library included all 15 annotated RNases from the *V. cholerae* genome, of which 2 were found to bind pGpG: VC0210 and VC0341 (Fig. 3, red dots). Additionally, the screen identified five ORFs that were not previously known to interact with pGpG: VC0371, VC2147, VC2459, VC2708, and VCA0593 (Fig. 3, orange dots). Sequence homology predictions indicate that four of these five proteins are predicted to interact with nucleic acids or nucleotides, whereas VCA0593 has no predicted function (Table S2). VC0341 is a homolog of Orn, which is a known exoribonuclease that cleaves two- to five-nucleotide-long RNAs (25). Because VC0341 was shown to bind in both the His-tagged and the His-MBP–tagged ORFeomes, it was chosen for further study.

Orn Binds to pGpG Specifically and Can Cleave It into GMP. To fully validate the interaction between Orn and pGpG observed in cell lysates, Orn from *P. aeruginosa* PA14 and *V. cholerae* were His-MBP tagged, purified, and assayed for pGpG binding by DRaCALA. pGpG bound both *P. aeruginosa* and *V. cholerae* Orn with fraction bounds of 0.32 ± 0.02 and 0.27 ± 0.01 in the absence of competitor (NC) (Fig. 4 *A* and *C*). Addition of excess unlabeled pGpG effectively competed radiolabeled pGpG binding, reducing the fraction bounds to 0.009 ± 0.008 and 0.03 ± 0.003 for *P. aeruginosa* and *V. cholerae* Orn ($P < 0.05$; Fig. 4 *A* and *C*). However, Orn binding to pGpG was not affected by the addition of excess c-di-GMP or any other guanine-containing nucleotides tested, indicating that Orn binds pGpG specifically (Fig. 4 *A* and *C*). Finally, Orn from *P. aeruginosa* and *V. cholerae* bound to pGpG with high affinity, with a K_d of 40 ± 2 and 25 ± 2 nM, respectively (Fig. 4 *B* and *D*).

Having demonstrated specific and high-affinity binding, we then investigated the ability of Orn to hydrolyze pGpG. Purified *P. aeruginosa* His-MBP-Orn degraded pGpG (Fig. 4*F*) into GMP within 10 s at room temperature. Orn belongs to the DEDDh subfamily of 3′ to 5′ exoribonucleases that have a highly conserved active site motif (39). The locations of the DEDDh active site residues were shown in the solved crystal structure of *Xanthomonas campestris* Orn (40), and an alignment of *P. aeruginosa* PA14 Orn with *X. campestris* Orn revealed the active site residues D11, E13, D111, H157, and D162 (Fig. S1). Single alanine point mutants in the signature motif of another DEDDh RNase, RNase T of *E. coli*, had significantly reduced catalytic activity (41). Therefore, we introduced single alanine substitutions into each residue of the DEDDh motif (D11A, E13A, D111A, H157A, and D162A) of *P. aeruginosa* Orn to assay for pGpG binding and degradation. All of the Orn variants bound pGpG (Fig. 4*E*) but failed to cleave pGpG (Fig. 4*F*). Taken together, these results demonstrate that

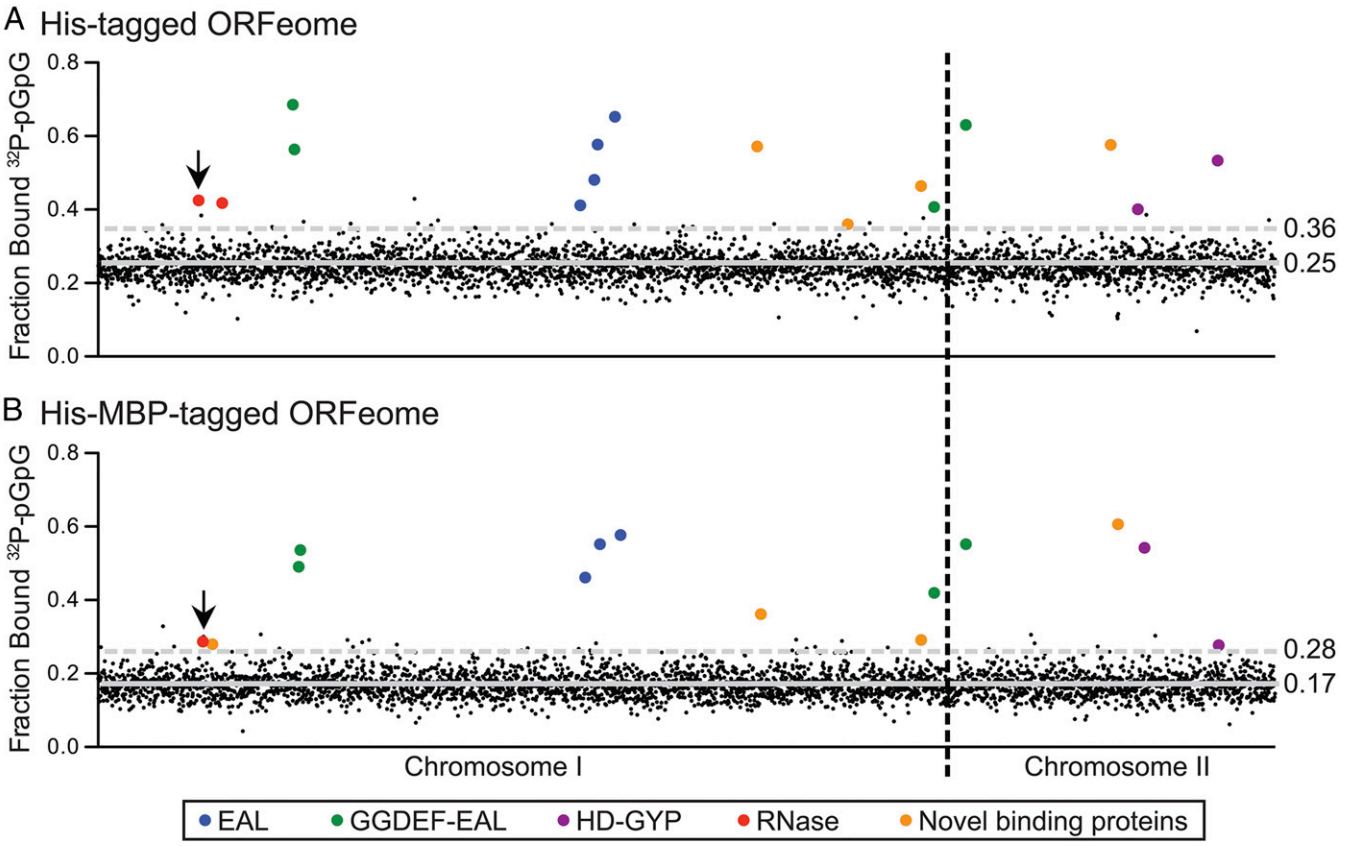

Fig. 3. A high-throughput DRaCALA screen to identify pGpG binding proteins from *V. cholerae*. The fraction bounds of ^{32}P-pGpG to each ORF from the *V. cholerae* (*A*) His-tagged or (*B*) His-MBP–tagged expression libraries. The ORFs are arranged in ascending numerical order by chromosome. The average fraction bound calculated for each library (solid gray line), and 3 SDs above the average (dotted gray line) are noted. Orn is marked by the black arrows. ORFs with fraction bounds below the cutoff or which were not validated are shown in small black circles. Colored circles indicate validated hits.

purified Orn binds pGpG with nanomolar affinity and requires an intact active site for pGpG hydrolysis activity.

Orn Is the Primary Enzyme Responsible for pGpG Degradation. Our results led us to ask whether Orn is the primary PDE-B responsible for turnover of pGpG in *P. aeruginosa*. An *orn* transposon mutant (*orn*::tn) and a control strain *cat*::tn (chloramphenicol acetyltransferase, which is not expected to affect pGpG hydrolysis) from the PA14 Transposon Library (26) were grown to midlog, lysed, and assayed for the ability to degrade radiolabeled pGpG. Lysates of the control *cat*::tn strain rapidly degraded pGpG (Fig. 5*A*). In contrast, the *orn*::tn strain showed a 10-fold reduced rate in pGpG cleaving ability, indicating that Orn is the primary enzyme involved in degradation (Fig. 5*A*). The *orn* mutant extracts still converted a small fraction of pGpG into GMP, indicating that there are additional proteins with PDE-B activity. Because purified HD-GYP domain phosphodiesterases from *P. aeruginosa* were shown to bind pGpG with higher affinity than c-di-GMP (21), we tested also pGpG degradation in cell lysates of transposon mutants of the two HD-GYP genes from *P. aeruginosa*. Lysates from PA4108::tn and PA4781::tn showed no reduction in rates of pGpG cleavage compared with *cat*::tn (Fig. 5*A*), so their individual contribution to pGpG turnover in vivo is less than Orn. To further validate the defect of the *orn*::tn strain, an in-frame deletion of *orn* was generated in *P. aeruginosa* PA14, and the cell lysate was analyzed for pGpG degradation. The *Δorn* strain showed a 25-fold reduced pGpG cleavage rate compared with the parental strain, consistent with the pGpG hydrolysis defect seen in the *orn*::tn strain (Fig. 5 *A* and *B*). Complementation with WT *orn* on an IPTG-inducible plasmid restored the ability to hydrolyze pGpG, whereas complementation with the catalytically inactive *orn* alleles did not (Fig. 5*C*). Addition of purified WT Orn from PA14 to the Δ*orn* lysate restored hydrolysis activity, whereas addition of the purified catalytically inactive proteins (D11A, E13A, D111A, H157A, and D162A) had no effect (Fig. 5*D*). Taken together, these results demonstrate that Orn is the primary enzyme responsible for removing pGpG in *P. aeruginosa*.

Aggregation and Biofilm Are Increased in an Orn Mutant and Dependent on the PEL Polysaccharide. We assayed the Δ*orn* strain for two phenotypes positively regulated by c-di-GMP: auto-aggregation (29) and biofilm formation (28). The auto-aggregation assay measures the ability of bacterial aggregates to settle. WT *P. aeruginosa* PA14 cultures remain in suspension, whereas the Δ*orn* strain formed larger aggregates that settled to the bottom of the culture tube (Fig. 6*A*). Complementation of Δ*orn* with active *orn* on a plasmid abolished aggregate formation, whereas complementation with catalytically inactive alleles did not (Fig. 6*B*). In a crystal violet microtiter plate assay for biofilm formation (42), cultures of WT *P. aeruginosa* PA14 formed less biofilm than Δ*orn*, with A_{595} readings of 0.84 ± 0.37 and 1.98 ± 0.73, respectively ($P < 0.05$; Fig. 6*C*).

In PA14, extracellular matrix products such as PEL exopolysaccharides are required for biofilm formation (43). Cyclic-di-GMP elevates the production of the PEL exopolysaccharides (28) by increasing transcription of the *pel* operon (27) and activating biosynthesis (30). Therefore, we generated a Δ*orn*Δ*pel* double deletion mutant to ask whether PEL is required for the increased

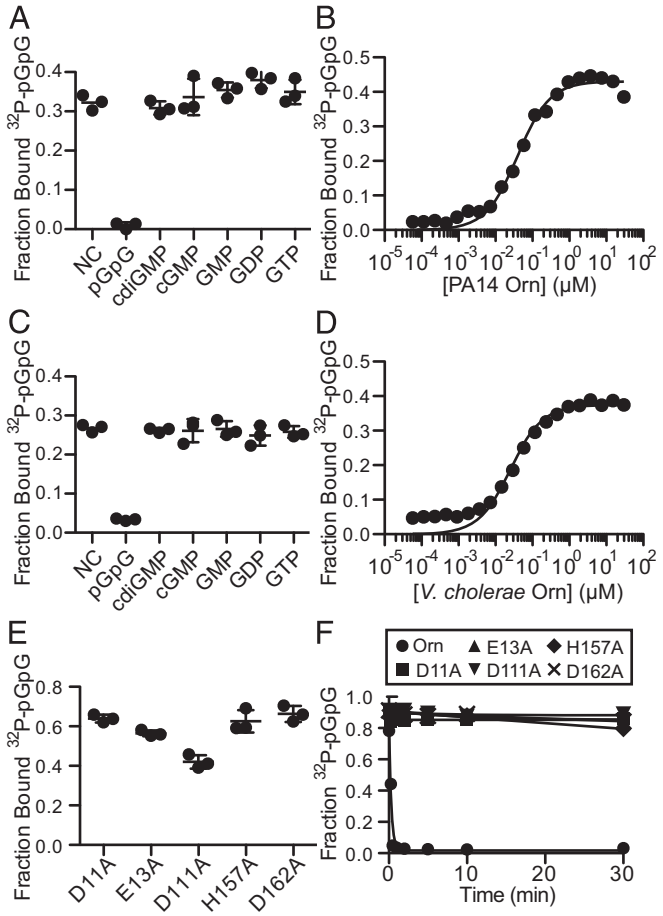

Fig. 4. Orn binds and hydrolyzes pGpG. Quantification of fraction bound of ^{32}P-pGpG to Orn from (*A*) *P. aeruginosa* PA14 or (*C*) *V. cholerae* in the presence of indicated competitors (250 μM). The dissociation constants (K_d) of ^{32}P- pGpG binding to Orn from (*B*) *P. aeruginosa* PA14 and (*D*) *V. cholerae* as determined by DRaCALA. (*E*) Quantification of the fraction bound of ^{32}P-pGpG to purified *P. aeruginosa* Orn active site mutants D11A, E13A, D111A, H157A, and D162A. (*F*) The rate of ^{32}P-pGpG hydrolysis by purified wild type Orn and active site mutants of *P. aeruginosa* Orn: D11A, E13A, D111A, H157A, and D162A. All data shown represent the average and SD of at least three independent experiments.

aggregation and biofilm formation we observe in the Δ*orn* mutant. The Δ*orn*Δ*pel* double mutant remained in suspension like the WT and the Δ*pel* single mutant cultures (Fig. 6*A*), indicating that PEL is required for the aggregation observed in the Δ*orn* strain. The *pel* operon is also known to be required for in vitro pellicle biofilm formation in *P. aeruginosa* PA14 (43). As expected, the Δ*pel* mutant was unable to form a pellicle biofilm in a microtiter plate assay, with a crystal violet A_{595} reading of 0.13 ± 0.02 compared with 0.84 ± 0.37 for WT ($P < 0.05$; Fig. 6*C*). The ability to form biofilm is also lost in the Δ*orn*Δ*pel* double deletion strain, which had an A_{595} reading of 0.21 ± 0.05 ($P < 0.05$ compared with WT; Fig. 6*C*). These data indicate that the increased aggregation and biofilm formation seen in the Δ*orn* strain is PEL dependent.

Another measure of elevated c-di-GMP levels is through the activity of the transcription factor FleQ, which leads to increased transcription from the *pel* promoter when bound to c-di-GMP (27). The *pel* promoter fused to *lacZ* (P_{pel}-*lacZ*) was integrated into the chromosome of both *P. aeruginosa* PA14 WT and Δ*orn* strains. These strains were grown to midlog and assayed for β-galactosidase activity. Approximately threefold increase in β-galactosidase activity was observed in the Δ*orn* strain compared with WT, with 563 ± 230 Miller units compared with 185 ± 64 Miller units, respectively ($P < 0.05$; Fig. 6*D*). Together, our results support the hypothesis that the loss of *orn* elevates c-di-GMP to promote c-di-GMP–regulated biofilms.

In additional support for the role of c-di-GMP in aggregation, overexpression of enzymes that either make or linearize c-di-GMP have opposing effects on aggregation in the Δ*orn* strain. Elevating c-di-GMP via overexpression of the DGCs *PA1107* and *wspR* increased aggregation. Conversely, decreasing c-di-GMP via expression of the PDE-As *PA2133* and *rocR* was unable to completely reverse bacterial aggregation (Fig. S2). These results indicate that because the Δ*orn* mutant lacks the ability to rapidly hydrolyze pGpG, it cannot complete degradation of c-di-GMP even when overexpressing EAL PDE-As.

Intracellular pGpG and c-di-GMP Are Elevated in the Oligoribonuclease Mutant. To confirm the presence of increased c-di-GMP and pGpG in the PA14 Δ*orn* strain, both nucleotides were directly detected by LC-MS/MS. WT and Δ*orn* cultures were grown midlog (OD_{600} = 0.6) and late-log (OD_{600} = 2.0), and the nucleotides were extracted for analysis. Both c-di-GMP and pGpG were detected in the PA14 WT and Δ*orn* mutant strains. At midlog, the Δ*orn* strain had 5.9-fold increased c-di-GMP compared with WT, with 2.86 ± 0.67 vs. 0.49 ± 0.08 μM, respectively ($P < 0.001$; Table 1). We also detect 6.6-fold more pGpG in the Δ*orn* strain than WT in midlog (70.8 ± 1.6 vs. 10.8 ± 1.4 μM; $P < 0.001$; Table 1). Lower concentrations of c-di-GMP and pGpG were detected from both strains at late-log, although both nucleotides remained higher in the Δ*orn* strain. At late-log, the Δ*orn* strain had 8.1-fold increased c-di-GMP compared with WT (0.65 ± 0.20 vs. 0.08 ± 0.01 μM, respectively; $P < 0.05$) and 6.6-fold increased pGpG compared with WT (26.3 ± 3.6 vs. 4.0 ± 1.0 μM, respectively, $P < 0.005$; Table 1). The above data confirm that pGpG and c-di-GMP are both elevated in *orn* mutants at both growth phases. All together, our results show that in

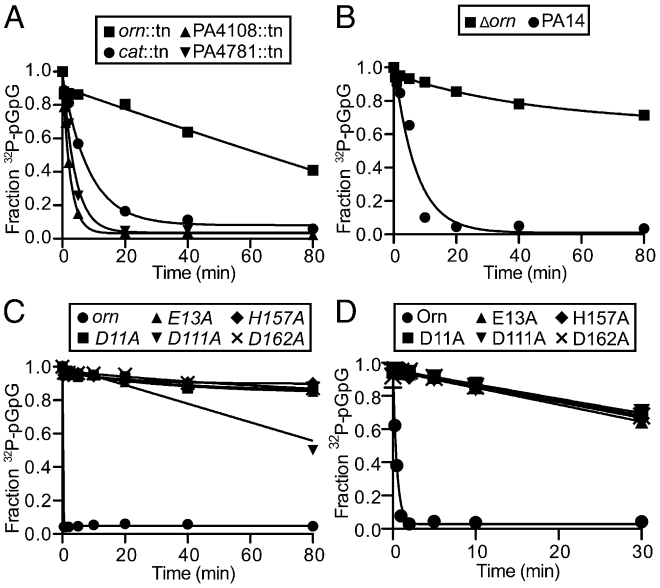

Fig. 5. PA14 *orn* mutants are defective in hydrolyzing pGpG. The rate of ^{32}P-pGpG cleavage by (*A*) whole cell lysates of *P. aeruginosa* PA14 transposon insertion strains *cat::tn*, *orn::tn*, *PA4108::tn*, or *PA4781::tn*, (*B*) whole cell lysates of *P. aeruginosa* PA14 or Δ*orn* in-frame deletion mutant, (*C*) whole cell lysates of *P. aeruginosa* Δ*orn* mutant complemented with WT or mutant alleles of *orn*, or (*D*) whole cell lysates of *P. aeruginosa* Δ*orn* with 100 nM of the indicated purified protein added. All data shown represent the average of triplicate independent experiments.

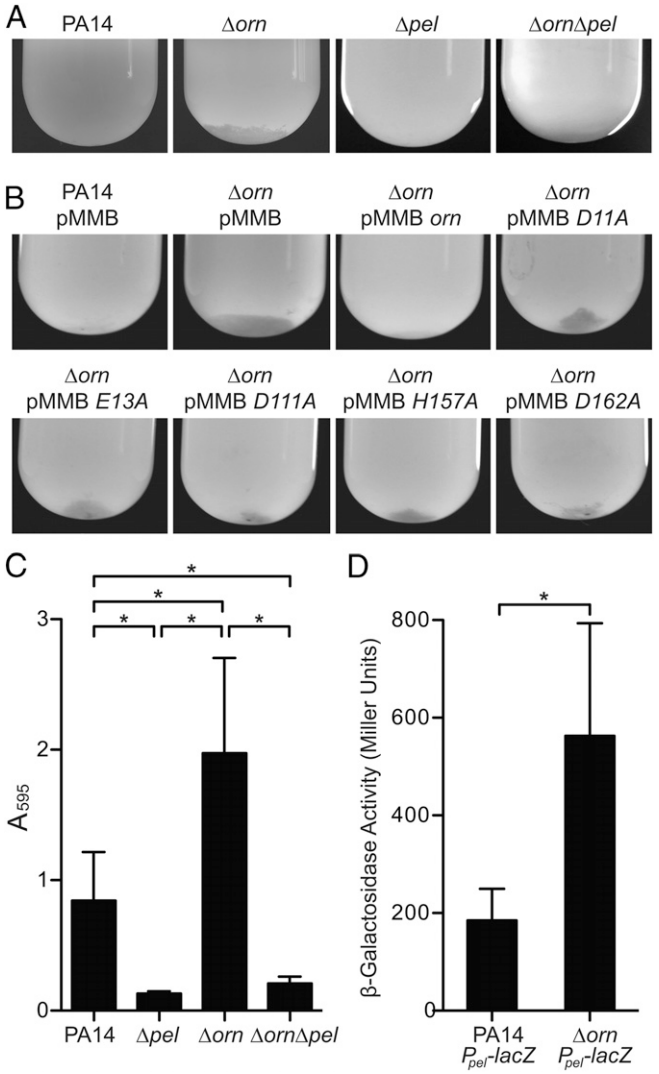

Fig. 6. Increased aggregation and biofilm formation in the *orn* mutant is PEL dependent. (*A*) Photograph of auto-aggregation assays of PA14, Δ*orn*, Δ*pel*, and Δ*orn*Δ*pel* mutants. (*B*) Photograph of auto-aggregation assays of PA14 and the Δ*orn* strain complemented with WT *orn* and active site mutant alleles. (*C*) Quantification of the biofilm formed after 24 h of static culture by the crystal violet assay by determining absorbance at 595 nm (A_{595}). A_{595} values results show the average and SD of triplicate independent experiments. (*D*) Miller assay showing β-galactosidase activity of WT and Δ*orn* strains containing a single copy of the *pel* promoter *lacZ* (*Ppel-lacZ*) reporter on the chromosome. $^*P < 0.05$ by Student unpaired two-tailed *t* test assuming equal variance for *C* and *D*.

addition to its known role degrading oligoribonucleotides (25), Orn is the major PDE-B that hydrolyzes pGpG in *P. aeruginosa*.

Discussion

Oligoribonucleases as PDE-Bs. Early characterization of c-di-GMP from the Benziman laboratory identified that c-di-GMP is linearized by PDE-As into pGpG, which is then degraded into two GMPs through the action of a presumed PDE-B (44). Through nearly three decades of c-di-GMP research that followed, the identity of the PDE-B remained unknown. We demonstrate here that the 3′-5′exoribonuclease Orn is the primary PDE-B in *P. aeruginosa*. The linearized product of c-di-GMP hydrolysis by PDE-As, pGpG, is a two-nucleotide-long RNA that matches the known substrates of Orn. We present several lines of evidence indicating that Orn is the primary PDE-B for c-di-GMP in *P. aeruginosa*: (*i*) Orn binds pGpG and not c-di-GMP, (*ii*) Orn rapidly degrades pGpG in vitro, (*iii*) lysates of *P. aeruginosa orn* mutants are greatly reduced for PDE-B activity, (*iv*) DEDDh catalytic residues used to degrade oligonucleotides are required for pGpG cleavage, and (*v*) loss of *orn* results in enhanced intracellular pGpG and c-di-GMP. This additional role for Orn is important because we demonstrate that the loss of Orn results in increased c-di-GMP and c-di-GMP governed phenotypes, likely due to accumulated pGpG inhibiting PDE-As as shown in our model (Fig. 7*A*).

Orn degrades short oligoRNAs regardless of sequence (45), raising the interesting possibility that it could degrade all linearized bacterial cyclic dinucleotides. In addition to c-di-GMP, two other cyclic dinucleotide signaling molecules have thus far been identified in bacteria. Cyclic di-AMP (c-di-AMP) is synthesized by diadenylate cyclases, which are widely distributed among bacterial species (46), and a hybrid cAMP-GMP is synthesized by DncV in *V. cholerae* (47) and an unknown cyclase in *Geobacter sulfurreducens* (48). Cyclic-di-AMP is linearized by HD domain and DHH-DHHA-1 domain phosphodiesterases (49, 50), and cAMP-GMP is linearized by HD-GYP proteins in *V. cholerae* (51). The linearized cyclic di-nucleotides could be hydrolyzed by Orn. However, not all species that use cyclic dinucleotides posses an Orn homolog (Fig. 7*B*). In a search of the clusters of orthologous group (COG) database, only Actinobacteria, Fibrobacteres, Betaproteobacteria, Deltaproteobacteria, Gammaproteobacteria, and a few unclassified species are predicted to encode Orn (52) (Fig. 7*B*). *Bacillus subtilis* has both c-di-GMP (53) and c-di-AMP signaling systems (54, 55) but lacks *orn*. Nevertheless, *B. subtilis* is capable of degrading two- to five-nucleotide-long RNAs using the potential Orn functional homologs NrnA, NrnB, yhaM, and RNase J1. All of these enzymes have oligoribonuclease activity and were able to partially complement an *E. coli orn* conditional mutant (56, 57). NrnA homologs are found in many bacteria that lack Orn (58). Additionally, another RNase with oligoribonuclease activity, NrnC, was recently identified in *Bartonella birtlesii* and is widely found in Alphaproteobacteria (59). Nearly all bacteria that encode diguanylate and diadenylate cyclases encode at least one RNase capable of degrading short oligoRNAs. Based on this genomic distribution, we predict these RNases are likely the primary PDE-Bs for hydrolyzing linearized cyclic dinucleotides into mononucleotides.

Our observation that residual PDE-B activity is present in mutants lacking *orn* indicates that other proteins can cleave pGpG. Proposed PDE-B candidates include the HD-GYP domain proteins, which were shown to bind pGpG with higher affinity than c-di-GMP in vitro and were capable of degrading pGpG (21). However, single transposon mutants in both of the HD-GYP domain proteins of *P. aeruginosa* PA14 did not show a defect in pGpG removal in our system, in contrast to the large defect observed for the *orn* mutant. Despite being shown to be

Table 1. Quantification of c-di-GMP and pGpG in PA14 and PA14 Δ*orn*

OD_{600}	PA14 (μM)	Δ*orn* (μM)	*P* value*	Δ*orn*/PA14
c-di-GMP				
0.6	0.49 ± 0.08	2.86 ± 0.67	0.007	5.9
2.0	0.08 ± 0.01	0.65 ± 0.20	0.02	8.1
pGpG				
0.6	10.8 ± 1.4	70.8 ± 1.6	2.4×10^{-6}	6.6
2.0	4.0 ± 1.0	26.3 ± 3.6	1.3×10^{-3}	6.6

Data shown are mean ± SD of three independent samples.
*P value was determined by Student unpaired two-tailed *t* test assuming equal variance.

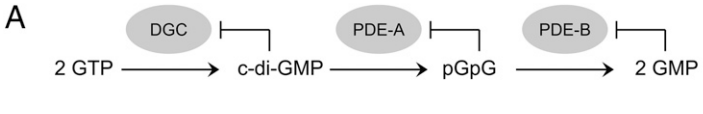

B

	Archaea	Synergistetes	Spirochaetes	Fusobacteria	Aquificae	Thermotogae	Actinobacteria	Chloroflexi	Cyanobacteria	Planctomycetes	Deinococcus-Thermus	Acidobacteria	Mollicutes	Chlamydiae	Clostridia	Bacilli	other Firmicutes	Bacteroidetes	Chlorobi	Alphaproteobacteria	Betaproteobacteria	Deltaproteobacteria	Epsilonproteobacteria	Gammaproteobacteria	other Bacteria
Total	83	5	7	5	8	7	74	9	31	6	6	6	10	6	49	33	6	55	5	75	52	28	11	103	31
Orn COG1949	0	0	0	0	0	0	64	0	0	0	0	0	0	0	0	0	0	0	0	0	47	8	0	101	4
NrnA COG0618	65	4	6	5	8	7	35	7	29	6	6	5	10	1	48	33	6	53	5	2	0	25	9	5	27
NrnB COG2404	52	4	0	1	3	0	0	0	2	0	0	1	0	0	2	5	0	0	1	3	12	4	10	5	6
GGDEF domain COG2199, COG2199	14	5	7	1	8	7	51	8	30	6	6	6	1	2	44	24	3	30	5	68	43	28	10	78	23
DisA domain COG1623, COG1624	42	5	7	5	8	7	50	7	31	6	6	3	7	6	48	33	6	46	1	0	0	27	0	0	25

Fig. 7. The distribution of RNases, GGDEF domain proteins, and diadenylate cyclase domain proteins. (*A*) A model showing the synthesis and degradation of c-di-GMP with the inclusion of pGpG-mediated feedback inhibition of EAL-domain PDE-As and Orn as a PDE-B. (*B*) A simplified phylogenetic tree of prokaryotic and archaeal species from the COG database and a table showing the number of species from each class that encodes the following proteins: Orn, NrnA, NrnB, GGDEF domains, and diadenylate cyclase (DisA) domains. The number of species were determined by a COG database search: Orn = COG1949; NrnA = COG0618; NrnB = COG2404; GGDEF = COG2199, COG3706; DisA = COG1623, COG1624.

essential in *E. coli* (60), *orn* mutants in *P. aeruginosa* are viable (26, 61), suggesting some functional redundancy. However, *P. aeruginosa* PA14 has no homologs of NrnA (56), NrnB (57), yhaM (expected value >1 in a protein BLAST search), RNase J1 (62), or NrnC (59). Other RNases may possess oligoribonuclease activity that partially compensates for the loss of *orn*. Our DRaCALA screen identified one other RNase, VC0419 (predicted based on homology to be RNase G), but purified VC0419 did not hydrolyze pGpG. Purified N-terminal His- and His-MBP–tagged RNase G from *E. coli* have been shown to be active in vitro against longer RNA substrates (≥10 nt) (63–65). RNase G has a 5′ monophosphosphate sensor pocket that binds 5′ monophosphorylated RNAs and is distinct from the active site (66, 67). It is possible that pGpG, which has a 5′ monophosphate, is bound by the 5′ sensor of VC0419, but cannot be accessed by the active site due to its short length. Other PDE-Bs responsible for residual pGpG cleavage may have been missed in our ORFeome binding screen. The screen is limited by the exogenous expression of targets in *E. coli*. For example, RNase E (VC2030) is structurally similar to RNase G and possesses a 5′ sensor pocket (67) and thus would be expected to bind pGpG, but SDS/PAGE analysis of the RNase E whole cell lysates from the ORFeome libraries showed the protein was poorly expressed. Another limitation of assaying whole cell lysates is that pGpG could be degraded by endogenous PDE-Bs from *E. coli*. Although Orn can rapidly degrade pGpG in whole cell lysates, we were able to detect binding in our DRaCALA screen because the buffer contained excess Ca^{2+} which prevents Orn activity (68). Future studies with a *P. aeruginosa* ORFeome library will seek to identify other RNases responsible for the residual non-Orn PDE-B activity.

Intracellular Concentration of pGpG and c-di-GMP. We were able to detect pGpG in both PA14 and the Δ*orn* mutant by LC-MS/MS. As expected, the level of pGpG in the Δ*orn* mutant was elevated compared with WT. The levels of pGpG detected in the Δ*orn* strain at both mid- and late-log are well above the K_d of RocR binding to pGpG. As a consequence, pGpG can compete for c-di-GMP binding to inhibit RocR activity, leading to the observed increase in c-di-GMP concentration. There are two potential sources of pGpG in the cell: linearization of c-di-GMP and normal RNA processing and turnover (69). Future studies will determine the relative contribution of each source. The detection of pGpG in the PA14 indicates a potential physiological role for pGpG in *P. aeruginosa* during normal growth conditions. Other positive hits from the ORFeome screen represent potential cellular receptors for other pGpG-regulated processes.

A previous study reported ∼11 μM of c-di-GMP in *P. aeruginosa* PAO1 grown to midlog in rich media (32). We detect ∼0.5 μM c-di-GMP for PA14 grown at midlog phase. The difference in c-di-GMP levels is likely due to differences between strains and estimations of cell size. The concentration of c-di-GMP for PA14 we detect is below the reported dissociation constants for *P. aeruginosa* c-di-GMP receptors, which are in the low micromolar range [Alg44 K_d = 5.6 μM (70), PelD K_d = 1 μM (30), and FleQ K_d = 15–25 μM (27)]. This level of c-di-GMP is consistent with PA14 cells behaving as motile, planktonic cells at midlog phase, which is indicative of reduced c-di-GMP signaling. However, the c-di-GMP concentration detected for the Δ*orn* mutant strain at midlog is ∼3 μM. The levels of c-di-GMP in the Δ*orn* mutant is sufficient to drive PelD activation, which is consistent with the requirement of the *pel* operon for biofilm formation and aggregation.

Cyclic-di-GMP Phenotypes in *orn* Mutants. The Δ*orn* strain formed more PEL-dependent biofilm and aggregates and had higher levels of pGpG and c-di-GMP. The connection between pGpG and elevated c-di-GMP is through pGpG inhibition of the PDE-As. The pGpG inhibition of PDE-A activity has also been observed for YfgF from *E. coli* (20). YfgF and RocR EAL domains are linked to different sensor domains and have different oligomer states (20, 71, 72), yet are both inhibited by pGpG. From our DRaCALA-based ORFeome screen, several other EAL and HD-GYP proteins also bind pGpG, suggesting that product inhibition by pGpG may be a general phenomenon. As a consequence, pGpG generated from c-di-GMP hydrolysis will act to extend c-di-GMP signaling unless a PDE-B is active to reduce the pGpG pool (Fig. 7*A*). As expected, deletion of the primary PDE-B

(*orn*) in *P. aeruginosa* resulted in the accumulation of c-di-GMP and increased biofilm formation and auto-aggregation. These observations will likely extend to other bacteria that use Orn homologs to degrade pGpG.

Orn may also be involved in other phenotypes regulated by c-di-GMP. Cystic fibrosis patients are chronically infected with mucoid strains of *P. aeruginosa*, leading to poor patient prognosis (73). The mucoid phenotype is due to high production of the alginate polysaccharide, which is synthesized by components of the *alg* operon (74). Cyclic-di-GMP regulates production posttranscriptionally by binding to the PilZ domain of Alg44 to activate alginate biosynthesis (70). Overexpression of the diguanylate cyclase PA1107 significantly enhanced alginate production in *P. aeruginosa* (70). In addition, transcription of the operon is regulated by several proteins, including the activator AlgB (75). A mucoid cystic fibrosis isolate FRD of *P. aeruginosa* becomes nonmucoid on deletion of *algB*, although the strain is still able to produce low levels of alginate (75). A genetic screen for suppressor mutants that restored alginate production of the *algB* mutant identified six transposon insertion mutants. Two of these insertions were in the *orn* gene (61). A possible explanation based on our model (Fig. 7*A*) is that the loss of *orn* resulted in pGpG accumulation, inhibition of PDE-A, and thus elevated c-di-GMP to allow for increased Alg44 activation and enhanced mucoidy. These observations indicate that the PDE-B must be present and highly active during c-di-GMP signaling termination to prevent pGpG-mediated PDE-A inhibition.

Materials and Methods

***V. cholerae* ORFeome Library pGpG Binding Screen.** Gateway destination vectors were generated from pET-19–derived expression vectors pVL791 (N-terminal His_{10} tag, carbenecillin resistance) and pVL847 (N-terminal His_{10}-MBP tag, gentamycin resistance). The Gateway destination cassette was amplified from pRFA and cloned in frame with the N-terminal tags to produce the gateway adapted vectors pVL791 GW and pVL847 GW. The *V. cholerae O1 biovar El Tor str. N16961* pDONR221 library was obtained from BEI Resources. The library was grown in 1.5 mL lysogeny broth (LB) in 2-mL, 96-well plates (Greiner) with kanamycin (50 mg/mL) selection, and the plasmids were isolated using the 96-well MultiScreen$_{HTS}$ Kit (Millipore). The ORFs were moved into the expression vector using LR-clonase enzyme II (Invitrogen) and introduced into chemically competent *E. coli* strain T7Iq (NEB) following the manufacturer's protocols. Recombinants were selected on LB agar plates containing either carbenecillin (50 mg/mL) or gentamycin (15 mg/mL). Multiple colonies from individual transformations were inoculated in LB M9-rich media in 96-well plate format and grown overnight with shaking at 30 °C with the appropriate antibiotic and then resuspended in 20% (vol/vol) glycerol and frozen at −80 °C.

E. coli T7Iq containing the *V. cholerae* ORFs were inoculated from frozen stocks in LB M9 rich media with the appropriate antibiotic in 96-well plate format, grown overnight with shaking at 30 °C, subcultured 1:50 into 1.5-mL fresh LB M9 media with antibiotic, and grown for 4 h at 30 °C with shaking; 1 mM IPTG was added to induce protein expression and cultures were grown for an additional 4 h. The induced culture was pelleted, and cells were resuspended in 1/10th volume of binding buffer (10 mM Tris, pH 8.0, 100 mM NaCl, 5 mM $CaCl_2$), as well as 10 μg/mL DNase, 250 μg/mL lysozyme, and 10 mM PMSF. Cells were lysed by three freeze/thaw cycles at −80 °C/21 °C. ORFeome whole cell lysates were stored at −80 °C until analysis by DRaCALA.

Binding of radiolabeled ligand to the ORFeome whole cell lysates was determined by DRaCALA as previously described (22, 23). Briefly, 16 pM ^{32}P-pGpG was added to the ORFeome whole cell lysate 96-well plates using a Multiflo Microplate Dispenser (BioTek) and then applied to nitrocellulose sheets (GE Healthcare) using a 96-well pin tool (V&P Scientific). The nitrocellulose was air dried and imaged using a Fujifilm FLA-7000 phosphorimager (GE), and the intensity of the DRaCALA spots was quantified using Fujifilm Multi Gauge software v3.0, and the fraction bounds were quantified (22, 23). To confirm that positive hits were not due to cross-contamination between plate wells, each positive hit was repicked from the expression library, and eight replicate single colonies were used to generate eight new whole cell lysates. These replicate lysates were compared with empty vector lysates for ^{32}P-pGpG binding by DRaCALA.

Strains and Culture Conditions. The primers, plasmids, and strains used in this study are listed in Tables S3–S5, respectively. The in-frame deletion of *orn* was generated in *P. aeruginosa* PA14 using a Flp-*FRT* recombination system (76). The ∼1-kb region upstream and downstream were PCR amplified and restriction digested to introduced these fragments into a pEX-Gn–based plasmid for making in-frame deletions as previously described (76). Deletions were verified by PCR. The *pel* promoter-*lacZ* fusion on a pCTX plasmid wa incorporated into the genomic *att* site as previously described (77).

The alanine point mutations were generated by QuikChange using the primers listed in Table S3. Silent mutations resulting in addition or removal of a restriction site were introduced to facilitate mutagenesis: these were the addition of an AfeI site in D11A and H157A, addition of an MscI site in D111A, and removal of EcoRV in D162A. The *orn* alleles from *P. aeruginosa* PA14 were cloned into pVL847 for purification and pMMB for complementation. The pMMB and pVL847 plasmids were maintained with gentamycin (15 mg/mL) and induced with 1 mM IPTG. Transposon mutants from the PA14 Non-Redundant Transposon Insertion Mutant Library (26) were maintained with gentamycin (15 mg/mL).

Protein Expression and Purification. His-MBP-RocR, His-MBP-Orn from *V. cholerae,* and His-MBP-Orn and His-MBP-Orn variants from *P. aeruginosa* were purified as previously described (23). Briefly, *E. coli* T7Iq strains or *E. coli* BL21(DE3) containing expression plasmids were grown overnight, subcultured in fresh media, and grown to OD_{600}∼1.0 when expression was induced with 1 mM IPTG. Induced bacteria were pelleted and resuspended in 10 mM Tris, pH 8, 100 mM NaCl, and 25 mM imidazole and frozen at −80 °C until purification. Proteins were purified over a Ni-NTA column followed by anion exchange on a Q-Sepharose column. Purified proteins were dialyzed twice against 10 mM Tris, pH 8, 100 mM NaCl, and 25% (vol/vol) glycerol, aliquoted, and frozen at −80 °C until use.

Whole Cell Lysate Generation. Overnight cultures of *P. aeruginosa* PA14 parental, mutant, or complemented strains were subcultured 1:50 into fresh LB media with appropriate antibiotic and IPTG conditions, grown to OD_{600} = 0.4 at 37 °C with shaking, resuspended in 1/10th volume of reaction buffer (10 mM Tris, pH 8, 100 mM NaCl, 5 mM $MgCl_2$), 10 μg/mL DNase, 250 μg/mL of lysozyme, and 10 mM PMSF, and lysed by sonication.

DRaCALA Measurement of Ligand Binding, Nucleotide Competition, and Dissociation Constant. The use of DRaCALA to probe protein–ligand interactions has been previously described (23). To assay binding, pure protein in binding buffer (10 mM Tris, pH 8.0, 100 mM NaCl, 5 mM $CaCl_2$) was mixed with radiolabeled ligand (4 pM ^{32}P-c-di-GMP or ^{32}P-pGpG), applied to nitrocellulose sheets, dried, imaged, and the fraction bound quantified (23). For competition assays, excess of unlabeled nucleotides were added to radiolabeled ligand and purified protein before analysis by DRaCALA (23). To measure K_d, twofold serial dilutions of purified His-MBP-Orn from either *P. aeruginosa* or *V. cholerae* were made in binding buffer (10 mM Tris, pH 8, 100 mM NaCl, 5 mM $CaCl_2$) and mixed with radiolabeled ligand and the fraction bound, and K_d was calculated as previously described (23).

Cell Lysate and Protein Activity Assays. The activity of whole cell lysates and purified proteins against ^{32}P-labeled substrates was measured by monitoring the appearance of ^{32}P-labeled products on TLC. The reactions were carried out at 37 °C in reaction buffer (10 mM Tris, pH 8, 100 mM NaCl, and 5 mM $MgCl_2$). At appropriate times, aliquots were removed and the reaction stopped by adding an equal volume of 0.2 M EDTA, pH 8, and heated at 98 °C for 10 min. Samples were spotted on polyethyleneimine-cellulose TLC plates (EMD Chemicals), dried, and developed in mobile phase consisting of 1:1.5 (vol:vol) saturated NH_4SO_4 and 1.5 M KH_2PO_4, pH 3.60. The TLC plate was dried and imaged using Fujifilm FLA-7000 phosphorimager (GE). The intensity of the radiolabeled nucleotides was quantified using Fujifilm Multi Gauge software v3.0.

Aggregation Assay. Cultures of *P. aeruginosa* strains were grown in 10 mL LB with appropriate antibiotic and IPTG conditions for 24 h at 37 °C with shaking. Cultures were imaged after 30 min of aggregate settling at room temperature.

Microtiter Plate Biofilm Assay. *P. aeruginosa* PA14 WT and mutant strains were grown overnight in LB at 37 °C with shaking. Overnight cultures were diluted 1:100 in LB and grown as static cultures in a 96-well polystyrene plate (Greiner) at 30 °C inside a humidified chamber for 24 h. The cultures were washed of planktonic cells and stained with crystal violet as previously described (42). The A_{595} was measured on a SpectraMax M5 spectrophotometer (Molecular Devices).

β-Galactosidase Reporter Assay. *P. aeruginosa* strains containing the reporter were grown overnight in LB at 37 °C with shaking. Overnight cultures were subcultured in LB and grown at 37 °C with shaking to midlog (OD_{600} = 0.5). The β-galactosidase activity was measured according to previously published methods (78).

Quantification of Intracellular c-di-GMP and pGpG. *P. aeruginosa* PA14 WT and Δ*orn* strains were grown overnight in LB at 37 °C with shaking, subcultured 1:100 in 20 mL LB, and grown at 37 °C with shaking to midlog (OD_{600} = 0.6) and late-log (OD_{600} = 2); 15 mL was pelleted by centrifugation, resuspended with 100 μL ice-cold extraction buffer, 40:40:20 (vol:vol:vol) MeOH, acetonitrile, and water with 0.1 N formic acid, incubated 30 min at −20 °C for lysis, and neutralized after a 30-min incubation with 4 μL 15% (wt/vol) NH_4NCO_3. Cellular debris was pelleted, and the supernatant was removed for desiccation by a Savant SpeedVac Concentrator (Thermo Scientific). Desiccated samples were suspended in 100 μL ultra-pure water, and insoluble material was pelleted at 21,000 × *g* using a table-top microcentrifuge at room temperature for 5 min. The resulting supernatant was filtered through a Titan syringe filter (PVDF, 0.45 μm, 4 mm) before quantification of c-di-GMP and pGpG. Quantification of c-di-GMP and pGpG in cellular extracts was performed using LC-MS/MS on a Quattro Premier XE mass spectrometer (Waters) coupled with an Acquity Ultra Performance LC system (Waters). Cyclic-di-GMP was detected in 10-μL injections of filtered extracts using previously described HPLC and MS parameters (79). For the detection of pGpG, filtered extracts were diluted 1:100 in ultra-pure water, and 10-μL injections of the diluted extracts were then analyzed with electrospray ionization multiple reaction monitoring in positive-ion mode at *m/z* 709.31 → 152.26. The MS parameters were as follows: capillary voltage, 2.8 kV; cone voltage, 34 V; collision energy, 40 V; source temperature, 120 °C; desolvation temperature, 350 °C; cone gas flow (nitrogen), 0 L/h; desolvation gas flow (nitrogen), 800 L/h; and collision gas flow (nitrogen), 0.2 mL/min. Chromatography separation was normal phase using a Waters BEH Amide 1.7 μm, 2.1 × 100-mm column with the following flow rates and gradient of solvent B (acetonitrile) to solvent A (50 mM ammonium acetate in ultra-pure water, pH 9.28): *t* = 0.00 min; 0.200 mL/min and A-1%:B-99%, *t* = 1.00 min; 0.300 mL/min and A-1%:B-99%, *t* = 2.00 min; 0.300 mL/min and A-10%:B-90%, *t* = 4.00 min; 0.400 mL/min and A-25%:B-75%, *t* = 5.01 min; 0.400 mL/min and A-99%:B-1%, *t* = 5.50 min; 0.400 mL/min and A-99%:B-1%, *t* = 5.51 min; 0.500 mL/min and A-99%:B-1%, *t* = 13.00 min; 0.500 mL/min and A-99%:B-1%, *t* = 13.01 min; 0.200 mL/min and A-1%:B-99%, *t* = 15.00 min; 0.200 mL/min and A-1%:B-99% (end of gradient). Standard curves for calculating c-di-GMP and pGpG concentrations in cellular extracts were generated by dissolving chemically synthesized c-di-GMP (Axxora) in water at concentrations of 250, 125, 62.5, 31.25, 15.62, 7.81, 3.91, and 1.95 nM and dissolving chemically synthesized pGpG (Axxora) in water at concentrations of 125, 62.5, 31.25, 15.62, and 7.81 nM. The intracellular concentrations of c-di-GMP and pGpG were determined by first calculating the total number of colony-forming units in each sample and multiplying this value by the intracellular volume of a single bacterium. The number of cells per sample were enumerated at OD_{600} = 0.6 and 2.0 for each strain by plating serial dilutions. The volume of one bacterium was estimated to be 4.3×10^{-1} fL, assuming the bacterium to be cylindrical in shape with spherical poles having an average length of 1.5 and 0.65 μm in diameter based on SEM image analysis (80). The total c-di-GMP and pGpG extracted in each sample were3 then divided by the total intracellular volume of the cells in the sample to provide the intracellular concentration of each analyte.

ACKNOWLEDGMENTS. We thank Dr. K. G. Roelofs for preparation of the *V. cholerae* ORFeome expression library, Dr. W. C. Winkler for critical reading of the manuscript, and Dr. D. J. Wozniak for helpful discussions. We thank Dr. M. Y. Galperin and J. R. Goodson for help with database searches for homologs. We appreciate assistance from Chen Zhang and the Michigan State University Mass Spectrometry Facility. M.W.O. was supported in part by a NIH/NIAID Training Grant in Host-Pathogen Interactions (T32-AI089621). V.T.L. was funded by National Institutes of Health (NIH) NIAID R21AI096083. C.M.W. was funded by National Science Foundation MCB1253684. H.O.S. was funded by National Science Foundation CHE0746446.

1. Römling U, Galperin MY, Gomelsky M (2013) Cyclic di-GMP: The first 25 years of a universal bacterial second messenger. *Microbiol Mol Biol Rev* 77(1):1–52.
2. Tal R, et al. (1998) Three cdg operons control cellular turnover of cyclic di-GMP in Acetobacter xylinum: Genetic organization and occurrence of conserved domains in isoenzymes. *J Bacteriol* 180(17):4416–4425.
3. Ryjenkov DA, Tarutina M, Moskvin OV, Gomelsky M (2005) Cyclic diguanylate is a ubiquitous signaling molecule in bacteria: Insights into biochemistry of the GGDEF protein domain. *J Bacteriol* 187(5):1792–1798.
4. Tamayo R, Pratt JT, Camilli A (2007) Roles of cyclic diguanylate in the regulation of bacterial pathogenesis. *Annu Rev Microbiol* 61:131–148.
5. Hengge R (2009) Principles of c-di-GMP signalling in bacteria. *Nat Rev Microbiol* 7(4): 263–273.
6. Römling U, Simm R (2009) Prevailing concepts of c-di-GMP signaling. *Contrib Microbiol* 16:161–181.
7. Krasteva PV, Giglio KM, Sondermann H (2012) Sensing the messenger: The diverse ways that bacteria signal through c-di-GMP. *Protein Sci* 21(7):929–948.
8. Simm R, Morr M, Kader A, Nimtz M, Römling U (2004) GGDEF and EAL domains inversely regulate cyclic di-GMP levels and transition from sessility to motility. *Mol Microbiol* 53(4):1123–1134.
9. Tamayo R, Tischler AD, Camilli A (2005) The EAL domain protein VieA is a cyclic diguanylate phosphodiesterase. *J Biol Chem* 280(39):33324–33330.
10. Schmidt AJ, Ryjenkov DA, Gomelsky M (2005) The ubiquitous protein domain EAL is a cyclic diguanylate-specific phosphodiesterase: Enzymatically active and inactive EAL domains. *J Bacteriol* 187(14):4774–4781.
11. Ryan RP, et al. (2006) Cell-cell signaling in Xanthomonas campestris involves an HD-GYP domain protein that functions in cyclic di-GMP turnover. *Proc Natl Acad Sci USA* 103(17):6712–6717.
12. Aldridge P, Paul R, Goymer P, Rainey P, Jenal U (2003) Role of the GGDEF regulator PleD in polar development of Caulobacter crescentus. *Mol Microbiol* 47(6):1695–1708.
13. Bobrov AG, Kirillina O, Perry RD (2005) The phosphodiesterase activity of the HmsP EAL domain is required for negative regulation of biofilm formation in Yersinia pestis. *FEMS Microbiol Lett* 247(2):123–130.
14. Tischler AD, Camilli A (2004) Cyclic diguanylate (c-di-GMP) regulates Vibrio cholerae biofilm formation. *Mol Microbiol* 53(3):857–869.
15. Simm R, Fetherston JD, Kader A, Römling U, Perry RD (2005) Phenotypic convergence mediated by GGDEF-domain-containing proteins. *J Bacteriol* 187(19):6816–6823.
16. Schirmer T, Jenal U (2009) Structural and mechanistic determinants of c-di-GMP signalling. *Nat Rev Microbiol* 7(10):724–735.
17. Chan C, et al. (2004) Structural basis of activity and allosteric control of diguanylate cyclase. *Proc Natl Acad Sci USA* 101(49):17084–17089.
18. De N, Navarro MV, Raghavan RV, Sondermann H (2009) Determinants for the activation and autoinhibition of the diguanylate cyclase response regulator WspR. *J Mol Biol* 393(3):619–633.
19. Yang CY, et al. (2011) The structure and inhibition of a GGDEF diguanylate cyclase complexed with (c-di-GMP)(2) at the active site. *Acta Crystallogr D Biol Crystallogr* 67(Pt 12):997–1008.
20. Lacey MM, Partridge JD, Green J (2010) Escherichia coli K-12 YfgF is an anaerobic cyclic di-GMP phosphodiesterase with roles in cell surface remodelling and the oxidative stress response. *Microbiology* 156(Pt 9):2873–2886.
21. Stelitano V, et al. (2013) C-di-GMP hydrolysis by Pseudomonas aeruginosa HD-GYP phosphodiesterases: Analysis of the reaction mechanism and novel roles for pGpG. *PLoS One* 8(9):e74920.
22. Corrigan RM, et al. (2013) Systematic identification of conserved bacterial c-di-AMP receptor proteins. *Proc Natl Acad Sci USA* 110(22):9084–9089.
23. Roelofs KG, Wang J, Sintim HO, Lee VT (2011) Differential radial capillary action of ligand assay for high-throughput detection of protein-metabolite interactions. *Proc Natl Acad Sci USA* 108(37):15528–15533.
24. Rolfs A, et al. (2008) Production and sequence validation of a complete full length ORF collection for the pathogenic bacterium Vibrio cholerae. *Proc Natl Acad Sci USA* 105(11):4364–4369.
25. Zhang X, Zhu L, Deutscher MP (1998) Oligoribonuclease is encoded by a highly conserved gene in the 3′-5′ exonuclease superfamily. *J Bacteriol* 180(10):2779–2781.
26. Liberati NT, et al. (2006) An ordered, nonredundant library of Pseudomonas aeruginosa strain PA14 transposon insertion mutants. *Proc Natl Acad Sci USA* 103(8): 2833–2838.
27. Hickman JW, Harwood CS (2008) Identification of FleQ from Pseudomonas aeruginosa as a c-di-GMP-responsive transcription factor. *Mol Microbiol* 69(2):376–389.
28. Hickman JW, Tifrea DF, Harwood CS (2005) A chemosensory system that regulates biofilm formation through modulation of cyclic diguanylate levels. *Proc Natl Acad Sci USA* 102(40):14422–14427.
29. Ueda A, Wood TK (2009) Connecting quorum sensing, c-di-GMP, pel polysaccharide, and biofilm formation in Pseudomonas aeruginosa through tyrosine phosphatase TpbA (PA3885). *PLoS Pathog* 5(6):e1000483.
30. Lee VT, et al. (2007) A cyclic-di-GMP receptor required for bacterial exopolysaccharide production. *Mol Microbiol* 65(6):1474–1484.
31. Robert-Paganin J, Nonin-Lecomte S, Réty S (2012) Crystal structure of an EAL domain in complex with reaction product 5′-pGpG. *PLoS One* 7(12):e52424.
32. Irie Y, et al. (2012) Self-produced exopolysaccharide is a signal that stimulates biofilm formation in Pseudomonas aeruginosa. *Proc Natl Acad Sci USA* 109(50):20632–20636.
33. Galperin MY, Nikolskaya AN, Koonin EV (2001) Novel domains of the prokaryotic two-component signal transduction systems. *FEMS Microbiol Lett* 203(1):11–21.
34. Beyhan S, Tischler AD, Camilli A, Yildiz FH (2006) Transcriptome and phenotypic responses of Vibrio cholerae to increased cyclic di-GMP level. *J Bacteriol* 188(10): 3600–3613.
35. Pratt JT, Tamayo R, Tischler AD, Camilli A (2007) PilZ domain proteins bind cyclic diguanylate and regulate diverse processes in Vibrio cholerae. *J Biol Chem* 282(17): 12860–12870.

36. Krasteva PV, et al. (2010) Vibrio cholerae VpsT regulates matrix production and motility by directly sensing cyclic di-GMP. *Science* 327(5967):866–868.
37. Srivastava D, Hsieh ML, Khataokar A, Neiditch MB, Waters CM (2013) Cyclic di-GMP inhibits Vibrio cholerae motility by repressing induction of transcription and inducing extracellular polysaccharide production. *Mol Microbiol* 90(6):1262–1276.
38. Srivastava D, Harris RC, Waters CM (2011) Integration of cyclic di-GMP and quorum sensing in the control of vpsT and aphA in Vibrio cholerae. *J Bacteriol* 193(22): 6331–6341.
39. Zuo Y, Deutscher MP (2001) Exoribonuclease superfamilies: Structural analysis and phylogenetic distribution. *Nucleic Acids Res* 29(5):1017–1026.
40. Chin KH, Yang CY, Chou CC, Wang AH, Chou SH (2006) The crystal structure of XC847 from Xanthomonas campestris: A 3′-5′ oligoribonuclease of DnaQ fold family with a novel opposingly shifted helix. *Proteins* 65(4):1036–1040.
41. Zuo Y, Deutscher MP (2002) Mechanism of action of RNase T. I. Identification of residues required for catalysis, substrate binding, and dimerization. *J Biol Chem* 277(51):50155–50159.
42. Merritt JH, Kadouri DE, O'Toole GA (2005) Growing and analyzing static biofilms. *Curr Protoc Microbiol* Chap 1:Unit 1B.3.1–1B.3.14.
43. Friedman L, Kolter R (2004) Genes involved in matrix formation in Pseudomonas aeruginosa PA14 biofilms. *Mol Microbiol* 51(3):675–690.
44. Ross P, et al. (1987) Regulation of cellulose synthesis in Acetobacter xylinum by cyclic diguanylic acid. *Nature* 325(6101):279–281.
45. Datta AK, Niyogi K (1975) A novel oligoribonuclease of Escherichia coli. II. Mechanism of action. *J Biol Chem* 250(18):7313–7319.
46. Corrigan RM, Gründling A (2013) Cyclic di-AMP: Another second messenger enters the fray. *Nat Rev Microbiol* 11(8):513–524.
47. Davies BW, Bogard RW, Young TS, Mekalanos JJ (2012) Coordinated regulation of accessory genetic elements produces cyclic di-nucleotides for V. cholerae virulence. *Cell* 149(2):358–370.
48. Kellenberger CA, et al. (2015) GEMM-I riboswitches from Geobacter sense the bacterial second messenger cyclic AMP-GMP. *Proc Natl Acad Sci USA* 112(17):5383–5388.
49. Huynh TN, et al. (2015) An HD-domain phosphodiesterase mediates cooperative hydrolysis of c-di-AMP to affect bacterial growth and virulence. *Proc Natl Acad Sci USA* 112(7):E747–E756.
50. Rao F, et al. (2010) YybT is a signaling protein that contains a cyclic dinucleotide phosphodiesterase domain and a GGDEF domain with ATPase activity. *J Biol Chem* 285(1):473–482.
51. Gao J, et al. (2015) Identification and characterization of phosphodiesterases that specifically degrade 3′3′-cyclic GMP-AMP. *Cell Res* 25(5):539–550.
52. Tatusov RL, Galperin MY, Natale DA, Koonin EV (2000) The COG database: A tool for genome-scale analysis of protein functions and evolution. *Nucleic Acids Res* 28(1): 33–36.
53. Gao X, et al. (2013) Functional characterization of core components of the Bacillus subtilis cyclic-di-GMP signaling pathway. *J Bacteriol* 195(21):4782–4792.
54. Oppenheimer-Shaanan Y, Wexselblatt E, Katzhendler J, Yavin E, Ben-Yehuda S (2011) c-di-AMP reports DNA integrity during sporulation in Bacillus subtilis. *EMBO Rep* 12(6):594–601.
55. Witte G, Hartung S, Büttner K, Hopfner KP (2008) Structural biochemistry of a bacterial checkpoint protein reveals diadenylate cyclase activity regulated by DNA recombination intermediates. *Mol Cell* 30(2):167–178.
56. Mechold U, Fang G, Ngo S, Ogryzko V, Danchin A (2007) YtqI from Bacillus subtilis has both oligoribonuclease and pAp-phosphatase activity. *Nucleic Acids Res* 35(13): 4552–4561.
57. Fang M, et al. (2009) Degradation of nanoRNA is performed by multiple redundant RNases in Bacillus subtilis. *Nucleic Acids Res* 37(15):5114–5125.
58. Postic G, Danchin A, Mechold U (2012) Characterization of NrnA homologs from Mycobacterium tuberculosis and Mycoplasma pneumoniae. *RNA* 18(1):155–165.
59. Liu MF, et al. (2012) Identification of a novel nanoRNase in Bartonella. *Microbiology* 158(Pt 4):886–895.
60. Ghosh S, Deutscher MP (1999) Oligoribonuclease is an essential component of the mRNA decay pathway. *Proc Natl Acad Sci USA* 96(8):4372–4377.
61. Woolwine SC, Wozniak DJ (1999) Identification of an Escherichia coli pepA homolog and its involvement in suppression of the algB phenotype in mucoid Pseudomonas aeruginosa. *J Bacteriol* 181(1):107–116.
62. Even S, et al. (2005) Ribonucleases J1 and J2: Two novel endoribonucleases in B.subtilis with functional homology to E.coli RNase E. *Nucleic Acids Res* 33(7): 2141–2152.
63. Tock MR, Walsh AP, Carroll G, McDowall KJ (2000) The CafA protein required for the 5′-maturation of 16 S rRNA is a 5′-end-dependent ribonuclease that has context-dependent broad sequence specificity. *J Biol Chem* 275(12):8726–8732.
64. Jiang X, Belasco JG (2004) Catalytic activation of multimeric RNase E and RNase G by 5′-monophosphorylated RNA. *Proc Natl Acad Sci USA* 101(25):9211–9216.
65. Jourdan SS, Kime L, McDowall KJ (2010) The sequence of sites recognised by a member of the RNase E/G family can control the maximal rate of cleavage, while a 5′-monophosphorylated end appears to function cooperatively in mediating RNA binding. *Biochem Biophys Res Commun* 391(1):879–883.
66. Jourdan SS, McDowall KJ (2008) Sensing of 5′ monophosphate by Escherichia coli RNase G can significantly enhance association with RNA and stimulate the decay of functional mRNA transcripts in vivo. *Mol Microbiol* 67(1):102–115.
67. Callaghan AJ, et al. (2005) Structure of Escherichia coli RNase E catalytic domain and implications for RNA turnover. *Nature* 437(7062):1187–1191.
68. Niyogi SK, Datta AK (1975) A novel oligoribonuclease of Escherichia coli. I. Isolation and properties. *J Biol Chem* 250(18):7307–7312.
69. Nickels BE, Dove SL (2011) NanoRNAs: A class of small RNAs that can prime transcription initiation in bacteria. *J Mol Biol* 412(5):772–781.
70. Merighi M, Lee VT, Hyodo M, Hayakawa Y, Lory S (2007) The second messenger bis-(3′-5′)-cyclic-GMP and its PilZ domain-containing receptor Alg44 are required for alginate biosynthesis in Pseudomonas aeruginosa. *Mol Microbiol* 65(4):876–895.
71. Chen MW, et al. (2012) Structural insights into the regulatory mechanism of the response regulator RocR from Pseudomonas aeruginosa in cyclic Di-GMP signaling. *J Bacteriol* 194(18):4837–4846.
72. Kulasekara HD, et al. (2005) A novel two-component system controls the expression of Pseudomonas aeruginosa fimbrial cup genes. *Mol Microbiol* 55(2):368–380.
73. May TB, et al. (1991) Alginate synthesis by Pseudomonas aeruginosa: A key pathogenic factor in chronic pulmonary infections of cystic fibrosis patients. *Clin Microbiol Rev* 4(2):191–206.
74. Chitnis CE, Ohman DE (1993) Genetic analysis of the alginate biosynthetic gene cluster of Pseudomonas aeruginosa shows evidence of an operonic structure. *Mol Microbiol* 8(3):583–593.
75. Goldberg JB, Ohman DE (1987) Construction and characterization of Pseudomonas aeruginosa algB mutants: Role of algB in high-level production of alginate. *J Bacteriol* 169(4):1593–1602.
76. Hoang TT, Karkhoff-Schweizer RR, Kutchma AJ, Schweizer HP (1998) A broad-host-range Flp-FRT recombination system for site-specific excision of chromosomally-located DNA sequences: Application for isolation of unmarked Pseudomonas aeruginosa mutants. *Gene* 212(1):77–86.
77. Hoang TT, Kutchma AJ, Becher A, Schweizer HP (2000) Integration-proficient plasmids for Pseudomonas aeruginosa: Site-specific integration and use for engineering of reporter and expression strains. *Plasmid* 43(1):59–72.
78. Miller JH (1992) *A Short Course in Bacterial Genetics: A Laboratory Manual and Handbook for Escherichia coli and Related Bacteria* (Cold Spring Harbor Laboratory Press, Plainview, NY).
79. Massie JP, et al. (2012) Quantification of high-specificity cyclic diguanylate signaling. *Proc Natl Acad Sci USA* 109(31):12746–12751.
80. Cole SJ, Records AR, Orr MW, Linden SB, Lee VT (2014) Catheter-associated urinary tract infection by Pseudomonas aeruginosa is mediated by exopolysaccharide-independent biofilms. *Infect Immun* 82(5):2048–2058.